Runtime Precoding: Enabling Multipoint Transmission in LTE-Advanced System-Level Simulations

MARTIN TARANETZ, (Student Member, IEEE), THOMAS BLAZEK, THOMAS KROPFREITER, MARTIN KLAUS MÜLLER, (Student Member, IEEE), STEFAN SCHWARZ, (Member, IEEE), AND MARKUS RUPP, (Fellow, IEEE)
Institute of Telecommunications, Vienna University of Technology, Vienna 1040, Austria

Corresponding author: M. Taranetz (martin.taranetz@nt.tuwien.ac.at)

ABSTRACT System-level simulations have become an indispensable tool for predicting the behavior of wireless cellular systems. As exact link-level modeling is unfeasible due to its huge complexity, mathematical abstraction is required to obtain equivalent results by less complexity. A particular problem in such approaches is the modeling of multiple coherent transmissions. Those arise in multiple-input-multiple-output transmissions at every base station but nowadays so-called coordinated multipoint (CoMP) techniques have become very popular, allowing to allocate two or more spatially separated transmission points. Also, multimedia broadcast single frequency networks (MBSFNs) have been introduced recently in long-term evolution (LTE), which enables efficient broadcasting transmission suitable for spreading information that has a high user demand as well as simultaneously sending updates to a large number of devices. This paper introduces the concept of runtime-precoding, which allows to accurately abstract many coherent transmission schemes while keeping additional complexity at a minimum. We explain its implementation and advantages. For validation, we incorporate the runtime-precoding functionality into the Vienna LTE-A downlink system-level simulator, which is an open source tool, freely available under an academic noncommercial use license. We measure simulation run times and compare them against the legacy approach as well as link-level simulations. Furthermore, we present multiple application examples in the context of intrasite and intersite CoMP for train communications and MBSFN.

INDEX TERMS Link abstraction, link quality model, runtime-precoding, 3GPP, LTE-A, Vienna LTE-A downlink system level simulator, MIESM, Vienna LTE-A downlink link level simulator, LTE transmission modes, coordinated multipoint, multimedia broadcast single frequency networks, high-user mobility.

I. INTRODUCTION

3gpp LTE-Advanced (LTE-A) is a key technology to meet the requirements of fourth generation mobile communication systems (4G), as specified by the ITU-R [1], [2]. Today, its limits are continuously pushed by academia, industry and standardization bodies. Typically, the potential performance of novel contributions is evaluated by extensive *simulations* under realistic conditions before gaining acceptance. To significantly reduce the complexity of such process, evaluations are often separated into two stages or levels of abstraction, referred to as *link level* and *system level*, respectively [3].

Link level simulations are applied for assessing the performance of the physical layer as well as those higher layer aspects that are directly related to the radio interface. Typically, only a single link is evaluated, including features such as synchronization, modulation and coding, channel fading, channel estimation and multi-antenna processing. It is by far too complex to simulate a substantial number of such links.

The focus of the present work is on system level, where performance evaluation requires to encompass a large number of network elements and upscales the number of interconnecting links. In this case, the main interest lies in network-related issues such as resource allocation, mobility management and network planning. Hence, computational complexity needs to be decreased substantially in order to make the problem feasible. A widely accepted solution is the application of *link abstraction models* [3] that specify the interaction between

link- and system level simulators and are further detailed in Section II. This structure is also expected to persist in simulation tools for the fifth generation of wireless cellular networks (5G) [4].

A. SURVEY ON EXISTING SIMULATION TOOLS

There are several ways to categorize existing system-level simulation tools. First, we may distinguish between simulators, which are implemented as 'modules' of a larger suite, and those, which are specifically designed for LTE-A [5]. Examples for the former include the *Riverbed SteelCentral NetModeler* (formerly *OPNET Modeler Suite*) [6], *OMNeT++* [7], *IT++* [8], *ns-2* [9], [10], *GNS3* [11], *openWNS* [12] and *Hurricane II* [13]. The main drawback of these solutions is their low level of detail, hence leaving most implementation work to the user. Consequently, results often lack accuracy and verification. On the other hand, technology-specific simulators are mainly developed by network operators and vendors, and are typically not intended for commercial distribution [5], [14]–[16]. Such tools yield a broad range of possibilities for parameter calibration and statistical evaluation. Thus, they are key instruments for the standardization process and the development of new technologies.

While these two classes of simulators largely vary in complexity, scalability and usability, probably the most relevant difference for scientific research is their accessibility. The authors strongly believe that *open access* is a key prerequisite for reproducible simulation studies. The short list of openly available, technology-specific approaches includes *LTE-Sim* [17], the tool presented in [16] and the *Vienna LTE-A downlink system level simulator*. While the first lacks of detailed Multiple-Input-Multiple-Output (MIMO) modeling, the second provides a rather limited set of features. In this work, we employ the *Vienna LTE-A downlink system level simulator* [18] (latest version: v1.8 r1375), subsequently referred to as *Vienna LTE-A simulator*, which is briefly introduced in the following.

B. THE VIENNA LTE-A DOWNLINK SYSTEM LEVEL SIMULATOR

The Vienna LTE-A simulator is implemented in object-oriented MATLAB[1] and is made openly available for download under an academic, non-commercial use license. Its rich set of features and easy adaptability has led to numerous publications from researchers all over the globe, including studies on energy-efficient cell-coordination schemes [20], handover algorithms in self-optimizing networks [21], and resource allocation techniques for femtocell networks [22] as well as for machine-to-machine communication [23]. On top of that, the *open accessibility* warrants the reproducibility of these contributions. Today (May 2015), the simulator counts more than 30 000 downloads and undergoes permanent peer-review from a substantially large online community.

[1]For further information, see [19].

With some 100 000 lines of code, employing a large forum with active users is the only method to guarantee its quality. For a comprehensive description, the interested reader is referred to [24].

C. CONTRIBUTIONS AND ORGANIZATION

This work is organized as follows. Section II briefly summarizes concepts for LTE-A physical layer modeling on system level. The centerpiece of this contribution is the presentation of a new *runtime-precoding* concept in Section III. Its innovation for openly available system level simulation tools lies in enabling the evaluation of scenarios where signals are coherently transmitted from multiple spatially separated transmission points while not compromising the complexity reduction as achieved by well established link abstraction models. For verifying the efficiency of our solution, we extend the link quality model of the Vienna LTE-A simulator by a runtime-precoding feature. We compare simulation run times as obtained with the enhanced- and the legacy model as well as with link level simulations. Section IV presents two example applications, showing the efficiency of intra- and inter-site Coordinated Multipoint (CoMP) schemes in high-speed train scenarios, and the implementation of eNodeB-coordinating entities in Multimedia Broadcast Single Frequency Networks (MBSFNs). Their investigation represent a novelty in the field of open-source LTE-A simulators, since both only became feasible with the proposed runtime-precoding concept. Section V concludes the work and outlines directions for future enhancements. The simulation assumptions throughout the paper are largely based on recommendations from 3GPP [25]–[27] and ITU-R [28], respectively. The source files for reproducing the results are openly available for download on our website www.nt.tuwien.ac.at/ltesimulator. Note that the proposed *runtime-precoding* concept is applicable to *any* system level simulation tool that employs the well accepted separation between link quality- and link performance model, as explained in Section II. Thus, the Vienna LTE-A simulator is just one out of many possible tools, which has been chosen to demonstrate the capabilities of the method.

II. PHYSICAL LAYER MODELING

This section provides a brief introduction to modeling concepts of the physical layer of LTE-A on system level. The LTE-A PHY procedures can conceptually be described as a Bit-Interleaved Coded
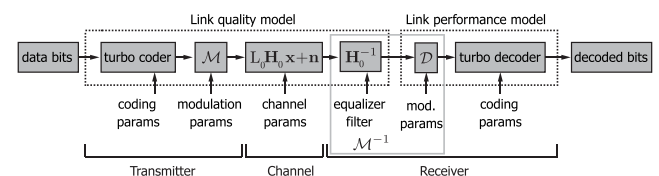

FIGURE 1. Separation of an LTE link into link quality- and link performance model. The link can equivalently be described as an LTE BICM transmitter-receiver chain [24].

Modulation (BICM)-system [24], as shown in Figure 1. It comprises a transmitter including channel coder, bit interleaver and modulator ($\mathcal{M}$). In LTE-A, coding and interleaving is achieved by a turbo-coder in combination with rate matching. The symbol mapping employs 4-, 16- and 64-QAM with Gray mapping, respectively. Signal propagation over an $N_{Rx} \times N_{Tx}$ MIMO channel is commonly modeled by slowly-varying, position-dependent macro-scale fading L_0, small-scale fading $\mathbf{H}_0$ and Additional White Gaussian Noise (AWGN). The matrix representation follows from the assumption that the cyclic prefix exceeds the channel length, hence omitting inter-symbol interference. The channel coefficients are typically calculated from a power-delay profile or a ray-based spatial channel model, such as the Winner model [29] or 3GPP's 3D model [30]. The receiver encompasses an equalizer filter and a demodulator ($\mathcal{M}^{-1}$) as well as a turbo decoder, which provides de-interleaving and channel decoding.[2]

The objective of the *link abstraction model* is to predict the performance of the presented LTE-A link, given a parameterization of the inputs. For simplification, the model can be divided into a *link quality-* and a *link performance model*, as indicated in Figure 1. The link quality model measures the quality of the received signal after equalization.[3] The link performance model translates this measure into Block-Error Ratio (BLER) and further into (area) spectral efficiency and effective throughput, based on the employed Modulation and Coding Scheme (MCS).
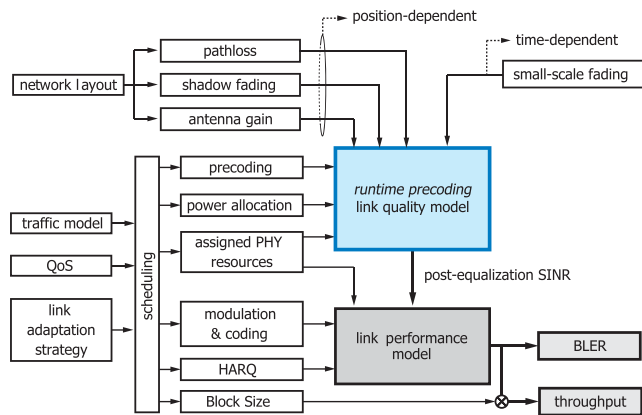

FIGURE 2. LTE link abstraction model with new *link quality model* as employed in the Vienna LTE-A downlink system level simulator v1.8 r1375.

The model in Figure 1 is a simplification of the actual link abstraction model, as it does not account for interference from other base stations. Its expansion to the whole network

is illustrated in Figure 2. The figure identifies the main components of the model as network layout, time-variant fading and scheduling. It also illustrates the corresponding input-output relations to the link quality- and link performance model, respectively.

The Vienna LTE-A simulator employs a Mutual Information based exponential SNR Mapping (MIESM) for the SINR-to-BLER mapping [32], [33], which already proved beneficial in Release 5 of UMTS [34], and was shown to outperform all other approaches (e.g., Exponential effective SINR mapping (EESM) [35]) in both complexity and performance. This method compresses the Signal-to-Interference-plus-Noise Ratio (SINR) values of the assigned Resource Blocks (RBs) for each User Equipment (UE) and 1 ms-long subframe (subsequently also denoted as Transmission Time Interval (TTI)) into an *effective SINR*, yielding an AWGN-equivalent representation in terms of mutual information. These SINR values are then mapped to a BLER by means of an AWGN BLER curve of the corresponding MCS. The curves are obtained from LTE link level simulations, thus forming the *only* computationally costly physical layer evaluation, which is required for the link abstraction model.

III. RUNTIME-PRECODING

In existing open-source system level simulation tools, UE association is limited to a single eNodeB with all antennas being mounted at the same site. In such scenarios, the fading as experienced over a MIMO link can be decomposed into a slowly varying, position-dependent macro-scale component and a faster changing small-scale component, as shown in Figure 2. Macro-scale fading is determined by the network layout and comprises antenna directivity, path loss and shadowing. Small-scale fading represents fast, frequency-selective channel variations over time. As explained in Section II, it is commonly modeled by a normalized[4] $N_{Rx} \times N_{Tx}$ channel matrix $\mathbf{H}_0$, where N_{Tx} and N_{Rx} denote the number of transmit- and receive antennas, respectively.

In the single-eNodeB-single-site case, the macro-scale parameter L_0 is a scalar, which is applied on all entries of $\mathbf{H}_0$. Thus, both L_0 and $\mathbf{H}_0$ can be computed *off-line* and *independently* from each other. Such separation further enables to determine the optimal precoder for each transmission rank a-priori with minimum loss of accuracy [24]. The *effective channel* $\mathbf{H} = \mathbf{G}\mathbf{H}_0\mathbf{W}$, which encompasses precoder $\mathbf{W}$ and receive filter $\mathbf{G}$, can be stored in *channel traces* and may be reused in all simulations with the *same MIMO setting*.

If the desired signal is received from *multiple* eNodeBs (e.g., in certain Coordinated Multipoint (CoMP) schemes, as indicated in Figure 3a) or from a single eNodeB with geographically separated antennas (e.g., in Distributed Antenna System (DAS)- and Remote Radio Head (RRH) deployments, as shown in Figure 3b), a-priori computation of the optimal

---

[2]In the current version of the Vienna LTE-A simulator, low complexity models for Zero Forcing (ZF)- and Minimum Mean Square Error (MMSE) receivers are available. The former approaches the average performance of an optimal receiver by exploiting Multi-User (MU) diversity, which is typically present in system level scenarios [31].

[3]Since the metric has to represent the quality of the input to the turbo decoder, the post-equalization Signal-to-Interference-plus-Noise Ratio (SINR) is a straightforward choice [24].

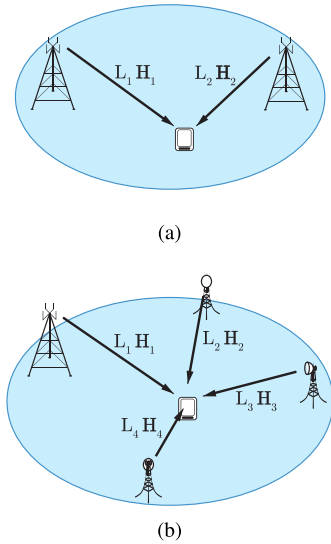[4]All entries of H_i have unit mean power in ensemble average.

FIGURE 3. Spatially distributed transmission points. (a) CoMP scenario. (b) eNodeB with RRHs.

precoders and the corresponding receive filters is no longer possible. In this case, only the normalized small-scale fading matrices $\mathbf{H}_i$ for each transmitter site can be pre-generated. The *composite channel* of the desired signal does not become available until *runtime*. It is obtained by stacking the matrices $\mathbf{H}_i$ from each transmitter-site and weighting them with the corresponding macro-scale losses, L_i, i.e.,

$$\mathbf{H}_0' = [L_1\mathbf{H}_1 \; L_2\mathbf{H}_2 \; L_3\mathbf{H}_3 \; \ldots]. \quad (1)$$

Then, the *effective channel* is calculated as $\mathbf{H} = \mathbf{G}\,\mathbf{H}_0'\,\mathbf{W}$. In this case, the optimal precoder, $\mathbf{W}$, and the corresponding receive filter $\mathbf{G}$ are determined *at runtime*. The challenge is to enable coherent signal reception from spatially distributed transmission points while keeping additional computational complexity at a minimum. Subsequently, we introduce the so called *runtime-precoding* method.

A. IMPLEMENTATION

The functionality of *runtime-precoding* is implemented in the UE's link quality model, as indicated in Figure 2. Its major building blocks are outlined in Algorithm 1. The model enables coherent signal reception from spatially distributed sources, *which can be selected at runtime*. At first, it collects the normalized small-scale fading channels and macro-scale losses for both desired and interfering signals. Then, the channels are stacked according to (1).

In the next step, the corresponding precoders are determined. By default, they may be chosen from a 3GPP standard-compliant codebook[5] [25]. Nonetheless, the availability of the *full channel at runtime* allows researchers to apply arbitrary precoders and beamformers,[6] yielding a

[5]There is no standardized method to determine the Precoding Matrix Indicator (PMI). The Vienna LTE-A downlink system level simulator employs a scheme that maximizes the mutual information between transmitted and received symbols [36].

[6]In general, beamforming strategies are found by solving multi-objective optimization problems [37].

Algorithm 1: Proposed UE link Quality Model With Runtime-Precoding Functionality.

Result: post equalization SINR
collect macroscopic path losses and normalized channel matrices from all transmitting sites;
calculate *composite desired channel* by stacking channel matrices of desired signal;
determine precoder or beamformer;
if *there are interferers* **then**
    calculate *composite interfering channels* by stacking channel matrices of interferers;
    determine precoders or beamformers for interfering channels;
else
    noise power only;
end
calculate receive filters and effective channel matrices;
determine post equalization SINR and store for link performance model;
calculate feedback based on actual channel;

---

profound novelty in open-source LTE-A system level simulation tools.[7]

B. PERFORMANCE EVALUATION

In this section, we evaluate the price to pay for enabling coherent multi-point transmission in system level simulations. For this purpose, we extend the UE link quality model of the Vienna LTE-A simulator by the runtime-precoding functionality according to Algorithm 1. Then we measure simulation run times with the new- and the legacy model. The results are compared with run times as obtained with the Vienna LTE-A Downlink Link Level simulator [39]. For a meaningful comparison, all simulations were carried out on the same hardware, an Intel(R) Core(TM) i7-3930K CPU @ 3.20 GHz, equipped with 32 GB of DDR3 1333 quad-channel RAM.

The common setup, which is employed in both link- and system level simulations, is summarized in Table 1. We carry out simulations with the LTE bandwidths $B = \{1.4, 3, 5, 10, 20\}$ MHz and the $N_{\text{Tx}} \times N_{\text{Rx}}$ antenna configurations $\{2 \times 2, 4 \times 2, 4 \times 1\}$ for various simulation lengths (measured in multiples of 1 TTI), in particular $N_{\text{TTI}} = \{100, 500, 1000\}$ on system level and $N_{\text{TTI}} = \{10, 100, 500\}$ on link level, respectively. Moreover, we perform system level simulations with $K = \{1, 10, 100\}$ UEs at a simulation length of 100 TTI. A round robin scheduler is employed.[8]

Figure 4 shows the obtained simulation run times. Each point was computed by averaging over ten simulation runs.

[7]The implementation of 3GPP's 3D channel model will enable the investigation of *elevation beamforming* and full-dimension MIMO [38].

[8]Note that the round robin scheduler does not increase in complexity with the number of physical RBs (i.e., increasing B). Other scheduling algorithms may have a considerable impact on the simulation run time in multi-user scenarios [24].

TABLE 1. Simulation parameters as employed for the simulation run time evaluation.

Parameter	Value
Frequency	2.14 GHz
Number of eNodeBs	1
Transmit power	5 W
eNodeB antenna gain pattern	omni-directional
LTE transmission mode	CLSM
Path loss in dB	$\max\left(10\log_{10}\left(\frac{4\pi d f}{c_0}\right)^2, 0\right)$
Shadow fading	none
Channel model	ITU-R Ped-A, block fading
Receiver type	zero forcing
Noise power spectral density	-160 dBm/Hz
UE position	random in circle with $R = 250$ m
UE antenna gain pattern	omni-directional
Traffic model	full buffer
Channel knowledge	perfect
Feeback	AMC: CQI, MIMO: PMI and RI
Feedback delay	3 TTI

It is observed that on system level the results scale approximately linearly with the simulation length N_{TTI}, the bandwidth B and the number of UEs K. Compared to this, the link level results exhibit a slightly non-linear scaling with B (note that on link level, only a single link is evaluated, i.e., $K = 1$). Both link- and system level run times show a non-linear dependence on the number of transmit- and receive antennas, N_{Tx} and N_{Rx}, respectively. From these observations, we can derive the following generic run time estimator (for a better understanding of the scaling with N_{Tx} and N_{Rx}, additional simulations with the MIMO configurations $\{2 \times 1, 4 \times 1\}$ were carried out):

$$T_{[\text{s}]}(N_{\text{TTI}}, B, N_{\text{Tx}}, N_{\text{Rx}}, K)$$

$$= (c_0 + N_{\text{TTI}} \cdot K \cdot B_{[\text{MHz}]} \cdot (c_1 N_{\text{Tx}} + c_2 N_{\text{Rx}} + c_3 N_{\text{Tx}} N_{\text{Rx}})$$

$$+ \ldots + N_{\text{TTI}} \cdot K \cdot B_{[\text{MHz}]}^2 \cdot (c_4 N_{\text{Tx}} + c_5 N_{\text{Rx}} + c_6 N_{\text{Tx}} N_{\text{Rx}}))$$

$$\times \ldots \times 1 \text{ s}, \tag{2}$$

where $B_{[\text{MHz}]} = B/10^6$ Hz. Next, we compute the coefficients $c_0, \ldots, c_6$ by linear least squares. The results are summarized in Table 2. Compared to the legacy link quality model, simulations with the new model require $1.25\times$ longer for initialization (represented by the coefficient c_0), which is still $52.5\times$ faster than link level simulations. It slightly decreases the scaling with $B_{[\text{MHz}]} \cdot N_{\text{Rx}}$ (referring to c_2) by $1.4\times$ while increasing c_3 (according to the scaling with $B_{[\text{MHz}]} \cdot N_{\text{Tx}} \cdot N_{\text{Rx}}$) by $2.7\times$. The latter term is of particular relevance for investigating massive MIMO scenarios with a large number of transmit antennas. On link level, c_2 (referring to a scaling proportional to $B_{[\text{MHz}]} \cdot N_{\text{Rx}}$) is $41.2\times$ larger than on system level, while $c_3 = 0$ (corresponding to the scaling proportional to $B_{[\text{MHz}]} \cdot N_{\text{Rx}} \cdot N_{\text{Tx}}$). On the other hand, the link level simulation run times scale with $N_{\text{Tx}} \cdot B_{[\text{MHz}]}^2$ and $N_{\text{Rx}} \cdot B_{[\text{MHz}]}^2$ (referring to c_4 and c_5), while system level simulations with both legacy- and new link quality model

exhibit no dependency on $B_{[\text{MHz}]}^2$, i.e., $c_4 = 0$, $c_5 = 0$ and $c_6 = 0$, respectively.[9]

IV. EXAMPLE APPLICATIONS

This section presents two examples for the application of the *runtime-precoding* enhanced UE link quality model. The simulation studies are carried out with the Vienna LTE-A simulator and, to the best of our knowledge, are the first of their kind with an openly-available LTE-A system level simulation tool.

A. HIGH-SPEED TRAIN SCENARIOS

This section investigates intra-site Joint Processing (JP) and inter-site Coordinated Scheduling (CS) [26] in the context of train communications. The particular scenario represents wireless access at high user mobility, which is becoming an increasingly important topic for commuting and traveling [40]–[42]. High-speed train scenarios have the specific feature of UEs moving in a deterministic manner and imposing a short but heavy traffic demand on the currently traversed cell. To support such traffic distribution, the application of RRHs is well suited [43], [44]. We apply the *runtime-precoding* enabled RRH feature of the Vienna LTE-A simulator to elaborate the impact of various RRH collaboration schemes on the UE performance. We assume direct links between the RRHs and the UEs, i.e., the trains are not equipped with roof-mounted relay nodes. This is a particularly realistic scenario for smaller countries such as most European, where mobile providers and train operators refrain from collaborating across country boarders.

1) SIMULATION SETUP

For simulations, we consider a representative segment of a railroad track, as shown in Figure 5. It comprises four equidistantly spaced sites, which are located along the tracks. Each site employs two RRHs pointing in opposite directions. For simplicity, only RRHs directed towards the train are taken into account. We assume the train to move between RRH_0 and RRH_1, and denote its location by the position of its center. Nodes RRH_{-1} and RRH_2 serve as dominant interferers.

Three ways of associating eNodeBs with RRHs are investigated:

- *Baseline:* All RRHs employ different cell IDs, i.e., are associated with different eNodeBs.
- *Coordination:* All RRHs are associated with different eNodeBs. Nodes RRH_0 and RRH_1 coordinate their transmission such that they do not interfere each other (e.g., by CS, thus effectively representing an example for *inter-site CoMP* [26]).
- *Cooperation:* Nodes RRH_0 and RRH_1 belong to the same eNodeB, thus acting as a DAS (as an example for *intra-site CoMP* [26]).

---

[9]A more detailed analysis of the link level simulation times shows that the non-linearity mainly arises from the symbol demapping and decoding, as described in Section II.
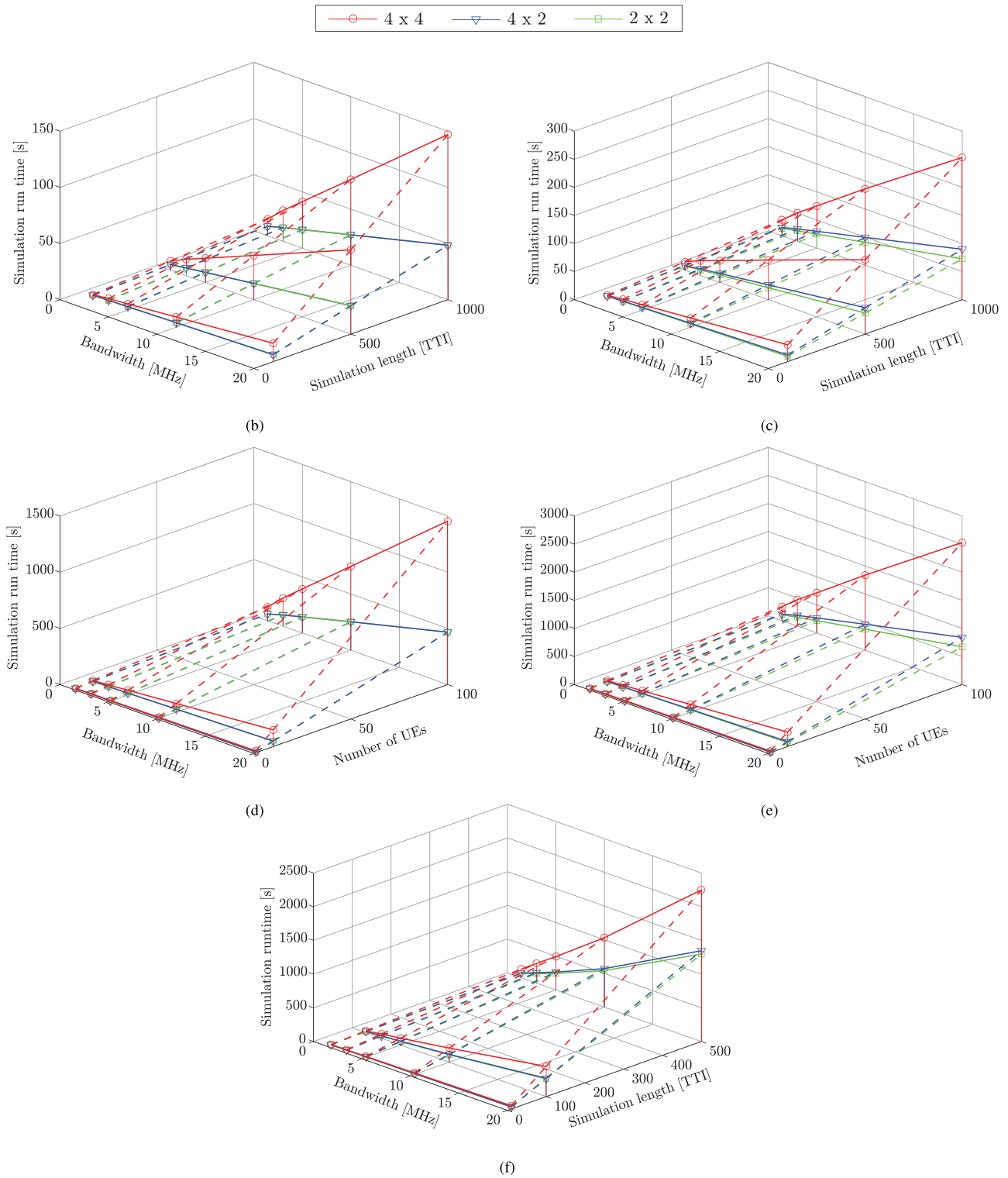
FIGURE 4. Simulation run times [s] for various LTE bandwidths [MHz], antenna configurations {$N_{TX} \times N_{RX}$} and number of UEs. (b) system level, *old* model, 1 UE. (c) system level, *new* model, 1 UE. (d) system level, *old* model, 100 TTIs. (e) system level, *new* model, 100 TTIs. (f) link level, 1 UE.

For a fair comparison, the total transmit power per eNodeB is limited to 40 W. Elaborated power allocation are omitted. In the cooperation case, serving- as well as interfering RRHs transmit with a power of 20 W. The parameters for simulation are summarized in Table 3. Transceiver impairments due to the high speeds, such as Inter-Carrier Interference (ICI), are taken into account by a *short block fading* model, which is explained in Appendix A.

TABLE 2. Coefficients for the runtime estimator in (2) as obtained by linear least squares. Values are provided for system level simulations with the legacy- and the new link quality model as well as for link level simulations.

| Simulation type	c_0	c_1	c_2	c_3	c_4	c_5	c_6
Legacy link quality model	0.8	0	$8.2 \cdot 10^{-4}$	$2.7 \cdot 10^{-4}$	0	0	0
New link quality model	1.0	0	$5.7 \cdot 10^{-4}$	$7.4 \cdot 10^{-4}$	0	0	0
Link level simulations	52.5	0	$235.0 \cdot 10^{-4}$	0	$2.3 \cdot 10^{-4}$	$11.0 \cdot 10^{-4}$	0
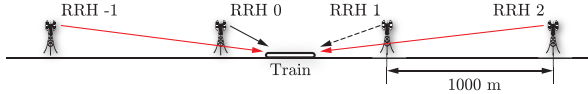
FIGURE 5. Representative segment for simulation of high-speed train scenario. RRHs are equidistantly spaced out along the tracks. The train moves between RRH_0 and RRH_1, RRH_{-1} and RRH_2 serve as interferers.

TABLE 3. Parameters for high-speed train scenario simulations.

Parameter	Value
Frequency	2.14 GHz
LTE bandwidth	$B = 20$ MHz
Inter-RRH distance	1000 m
eNodeB transmit power	40 W
Antennas per RRH	2
LTE transmission mode	CLSM
Antenna gain in dB	$A(\theta) = -\min\left(12\left(\frac{\theta}{70°}\right), 20\,\text{dB}\right)$
Minimum coupling loss	70 dB
Path loss model	$128.1 + 37.6 \log_{10}(R)$, R in km
Shadow fading model	correlated log normal, $\sigma = 10$ dB
Channel model	ITU-R Veh-A, *short* block fading
Receiver type	zero forcing
Noise power spectral density	-174 dBm/Hz
Receiver noise figure	9 dB
Train speed	250 km/h
Train length	200.84 m
Train penetration loss	constant, 30 dB
Active UEs	$K = 230$
UE distribution within train	uniform
Antennas per UE	1
Traffic model	full buffer
Scheduler	proportional fair
Channel knowledge	perfect
Feedback	AMC: CQI, MIMO: PMI and RI
Feedback delay	3 TTI
RRH backhaul connection	radio over fiber, no delay
Simulation length in TTI	$N_{\text{TTI}} = 100$
Number of simulation runs	24 per train position

2) SIMULATION RESULTS

Figure 6 provides results in terms of train average spectral efficiency, i.e., the mean over all passengers at a certain train position.[10] It is observed that the cooperation scheme universally achieves the highest performance while completely avoiding hand-overs in the region of interest. Coordination among RRHs yields a lower performance, particularly in the middle between two RRHs. Note, however, that in practical scenarios such scheme is typically far less complex than cooperation. This stems from the fact that only

[10]We evaluated 24 train locations between 600 m and 1400 m. For each location, 24 simulation runs with a length of 100 TTIs were carried out.
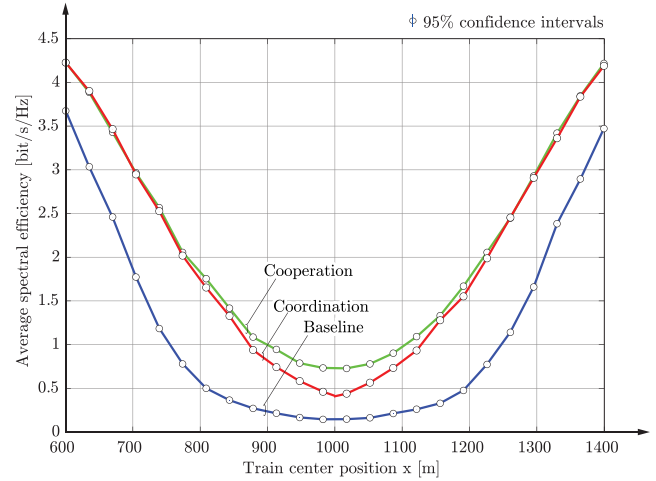
FIGURE 6. Train average spectral efficiency [bit/s/Hz] versus train position for three RRH collaboration schemes.

control data has to be exchanged among the eNodeBs. The baseline scenario yields the worst performance due to the presence of a strong interferer. Such studies are valuable for network providers, to minimize the cost of necessary installations along the tracks. Due to the short simulation length of 100 TTI (0.1 s), effects of hand-overs are not considered. They may completely be prevented by the concept of *moving cells*, as reported in [45].

3) SIMULATION RUN TIMES

Employing the same hardware as utilized for the performance analysis in Section III-B, we measure the system level simulation run times for each of the three RRH association scenarios. The results are provided in Table 4. They were obtained by averaging over 24 train positions and 24 simulation runs for each position. It is found that the new link quality slows down simulation by a factor of 3.7 compared to the legacy model. On the other hand, it enables to evaluate the cooperation scheme in the first place.

TABLE 4. System level simulation run times [s] as required for evaluating various RRH association schemes in train scenarios.

Simulation type	*Baseline*	*Coord.*	*Coop.*
Legacy link quality model	66	66	–
New link quality model	242	242	277

TABLE 5. Simulation parameters for MBSFN scenario.

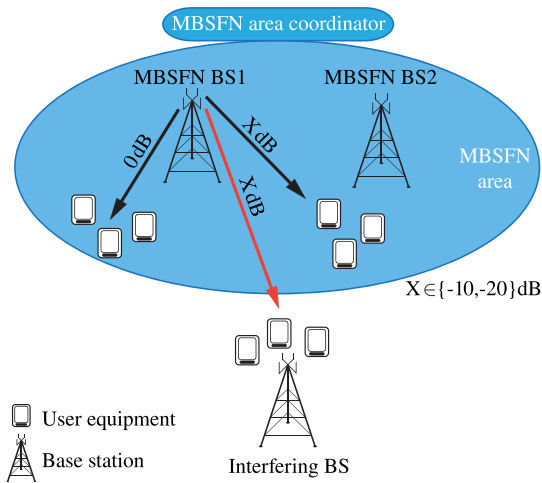| Parameter	Value
Frequency	2.14 GHz
LTE bandwidth	$B = 5$ MHz
Macroscopic path loss	fixed
Shadow fading	none
Channel model	ITU-R Veh-A, block fading
Receiver type	zero forcing
Average noise power	-13 dB
Transmission rate	fixed, 1.2 bit per channel use (CQI 6)
Scheduler	round robin multicast group scheduler
Cyclic prefix	extended
Simulation length in TTI	$N_{\mathrm{TTI}} = 10\,000$

FIGURE 7. Example scenario for comparison of MBSFN simulations on link level and system level.

B. MULTIMEDIA BROADCAST SINGLE FREQUENCY NETWORKS

Employing cellular networks to broadcast information to a multitude of UEs in parallel, enabling services such as mobile radio and TV, is a desire that persists already since the introduction of Multimedia Broadcast Multicast Services (MBMS) with Release 6 of UMTS (March 2005). In LTE, the concept has been extended to enhanced MBMS (eMBMS), including Multimedia Broadcast Single Frequency Networks (MBSFNs) as a main feature. By grouping several eNodeBs to broadcast the same information over potentially large geographic areas, MBSFNs allow to form so-called *multicast/broadcast areas*, as indicated in Figure 7. Within such area, interference between eNodeBs is not only avoided, but even exploited as useful signal. The resulting peak data rates and network capacities enable high-quality video broadcasting and low latency transmissions [2]. Currently, interest in enhanced MBMS (eMBMS) and MBSFNs is increasing within the 3GPP, as they allow to efficiently spread information that has a high user demand, e.g., at large events (venue casting) or during peak hours, as well as to simultaneously update a vast amount of devices, which is expected to become a common use case with the advent of the Internet of Things [46]. Moreover, they enable

public safety services, road safety applications, as well as tasks of fleet control with LTE-A.

1) IMPLEMENTATION

The support of MBSFN in the Vienna LTE-A simulator required some significant modifications of the program code. Signals that previously counted as interference, now have to be considered as useful signals in the SINR calculation. However, it is not expedient to simply add up the received powers from all the eNodeBs within the MBSFN area, since these base stations broadcast the same information synchronously. Thus, instead of adding signal powers, it is necessary to add the channel matrices $\mathbf{H}_i$ of all eNodeBs $i \in \mathcal{A}$ within the MBSFN area $\mathcal{A}$, i.e., $\mathbf{H}_{\mathrm{MBSFN}} = \sum_{i \in \mathcal{A}} \mathbf{H}_i$. This became feasible with the *proposed runtime-precoding concept* as outlined in Section III. In an additional step, the MBSFN base stations are filtered out from the interfering eNodeBs and the corresponding effective MBSFN channel matrices for multicast UEs are determined.

The support of MBSFN further requires a new element in the networking hierarchy, termed *MBSFN area coordinator*. It determines the resource allocation for all eNodeBs within the corresponding MBSFN area during subframes that are utilized for multicast transmission. UEs within the MBSFN area can subscribe to multicast groups in order to receive certain multicast messages. The task of the MBSFN area coordinator is to decide on the schedule of these multicast groups within the MBSFN subframes. This group schedule is then forwarded to the corresponding MBSFN eNodeBs, which signal the information to the multicast UEs. As an example, a round robin multicast group scheduler has been implemented in the Vienna LTE-A simulator.

To enable LTE-A standard-compliant MBMS/MBSFN simulations, a few further restrictions have to be considered in the simulator. Multicast transmissions within MBSFN areas always apply the extended cyclic-prefix of LTE-A, in order to avoid inter-symbol interference due to the increased delay spread of the effective MBSFN channel. Furthermore, reference-symbols are more densely placed in MBSFN subframes, to compensate for the larger frequency selectivity of the effective channel due to the increased delay spread. Basically, on system level, both of these changes cause a difference in the number of available resource elements compared to unicast transmission and are taken into account when calculating the throughput.

2) COMPARISON OF MBSFN SIMULATIONS ON LINK LEVEL AND SYSTEM LEVEL

For validation of the system level MBSFN implementation, we cross-compare with results from link level simulations. A simple example scenario as illustrated in Figure 7, is employed. A larger network cannot be simulated on link level due to computational complexity issues. In this scenario, we consider a single MBSFN area consisting of two MBSFN eNodeBs and serving a total number of six UEs. An additional unicast base station serves three UEs and acts as out-of-area interferer. The direct link between a UE and
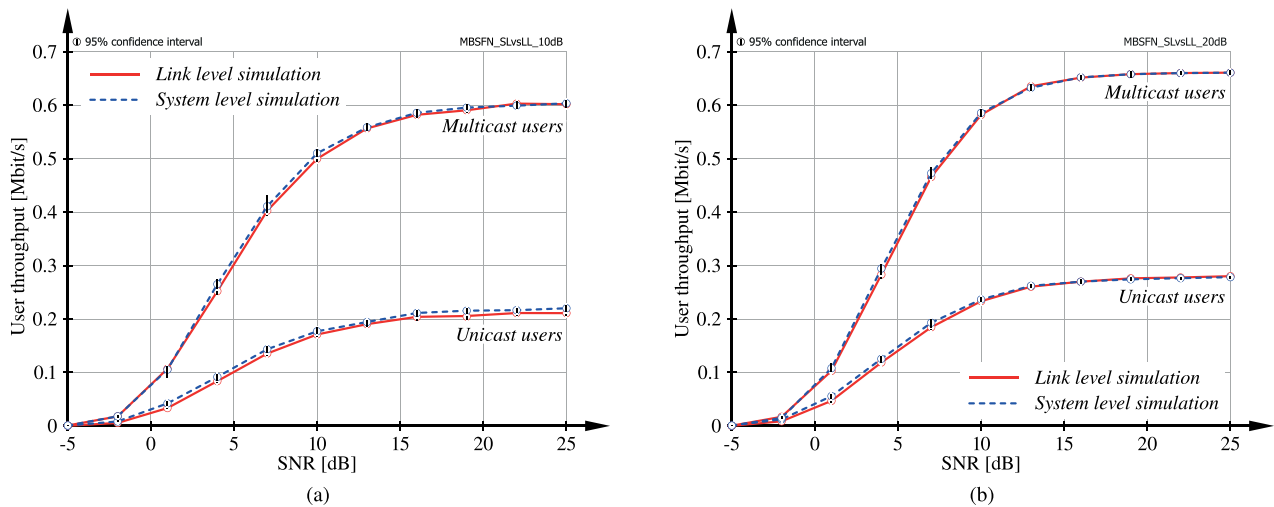
FIGURE 8. Throughput [Mbit/s] as achieved by multicast and unicast UEs. Results are obtained from link- and system level simulations with 95 % confidence intervals. (a) Signal to interference ratio 10 dB. (b) Signal to interference ratio 20 dB.

its associated eNodeB has an average gain of $0\,$dB, whereas the link to other UEs experiences an average gain of X dB, with $X \in \{-10, -20\}$. We employ a fixed transmission rate of approximately 1.2 bit per channel use (corresponding to Channel Quality Indicator (CQI) 6), to avoid the impact of transmission rate adaptation in the results.

The results of the link level simulation (red solid) and the system level simulation (blue dashed) are shown in Figure 8. At high interference power, i.e., $X = -10$ dB, we observe that there is a marginal mismatch between link and system level results, as the system level simulator slightly overestimates the performance. This is caused by the fact that, on system level, interference is considered Gaussian distributed, which is an over-simplification since the interference signals are taken from a finite symbol alphabet (4-QAM). However, when simulating larger networks, as is commonly the case on system level, the law of large numbers validates the application of this Gaussian approximation. Despite the small size of the scenario, cross-comparing the simulation times of system- and link level exhibit a speed-up of about $3.5\times$.

V. CONCLUSION AND FUTURE WORK

This work presented the concept of *runtime-precoding* that enables the simulation of coherent signal transmission from spatially separated transmission points on system level. Our approach only alters the link quality model while preserving the complexity gains as achieved by state of the art link abstraction models. The price to pay for enabling coherent multi-point transmission turned out to be an additional upscaling of the simulation run time which is proportional to the product of the number of transmit- and receive antennas, respectively. On the other hand, the run times showed a linear- rather than a quadratic growth with the bandwidth, the latter being observed in link level simulations. Two examples for the application of runtime precoding, inter- and intra-site CoMP in fast train scenarios and MBSFNs, were studied.

While the results for a simple MBSFN scenario were highly consistent with link level simulations, achieving a simulation run time speed-up of about $3.5\times$, such comparison was not possible at all for the CoMP scenarios, as the large number of network elements restricted evaluations to system level. The runtime-precoding feature slowed down the simulations of the coordinated-scheduling scenario by $3.7\times$. On the other, it enabled the investigation of the joint transmission scheme in the first place. Thus, enhancing the link quality model by runtime-precoding provides a convenient tool for simulating large-scale coherent multi-point transmission scenarios, where evaluation on link level is no longer feasible due to complexity issues. The source code, including all the presented new features and examples, is freely available for download under an academic, non-commercial use license. Our future work is directed towards 3-dimensional channel models [30], which will enable the investigation of elevation beamforming and full-dimensional MIMO [38].

APPENDIX
MODELING HIGH USER-MOBILITY IN THE VIENNA LTE-A SYSTEM LEVEL SIMULATOR

The LTE-A standard is designed to support reliable communication with users moving at velocities as high as $500\,$km/h [2]. At such high speeds, several transceiver impairments such as channel estimation errors [47] and ICI between Orthogonal Frequency Division Multiplexing (OFDM) subcarriers [48], become non-negligible. These and similar imperfections were, however, not considered in legacy versions of the Vienna LTE-A simulator.

A. IMPLEMENTATION

In this section, we explain the extension of the Vienna LTE-A simulator to account for the suboptimal transceiver operation. In a first step, we investigate the impact of ICI on the performance of the system. Then, we show that a similar

approach can be applied to consider other imperfections as well. The basic requirement is that the impairments can be modeled sufficiently well as *additional Gaussian noise* and are treated as such by the receivers. Although such assumptions do not hold in general, they were found to accurately resemble link level simulations as well as measurements for the considered LTE-A scenarios.

The impact of ICI on the performance of OFDM systems has been reported in several publications. In [48], a relatively simple expression for the average ICI power as experienced by an OFDM transmission over a fast and frequency selective Rayleigh fading channel is derived. This expression is particularly suitable for the Vienna LTE-A simulator, as it only depends on the maximum Doppler shift of the channel and can hence be evaluated easily. However, the model is not very precise as it employs an average over the fading channel rather than using the current realization.

In the Vienna LTE-A simulator, the ICI power can be taken into account by modifying the post-equalization SINR calculation in the UE link quality model (conf. Algorithm 1). In particular, we consider the ICI power as additional Gaussian noise and add it on top of the already existing thermal noise. Before, however, it is necessary to account for the macro-scale fading as well as the UE power allocation by multiplying the ICI power as obtained from [48] with the corresponding fading parameters (pathloss, shadow fading, antenna gain) as well as the transmit power. In case that RRHs are employed, we assume the ICI power contributions from the antenna arrays to be statistically independent and simply accumulate the individual values.

B. SIMULATIONS

The performance of this simple ICI model can be investigated and verified by comparing the outcome of system level simulations to the results as obtained with the Vienna LTE-A link level simulator [39]. The link level simulator supports a fast fading channel model, in which the channel varies in between OFDM samples ($0.52\,\mu$s sampling rate at 1.4 MHz bandwidth) and causes ICI. In contrast, the system level simulator applies a block fading channel model, where the channel varies only from one LTE subframe (14 OFDM symbols, 1 ms duration) to the next. With both simulators, we evaluate a single-UE-single-eNodeB scenario as specified in Table 1. Both eNodeB and UE are equipped with one antenna and the transmission takes place with a fixed transmission rate of approximately 5.5 bit per channel use (corresponding to CQI 15). To highlight the impact of ICI, an unrealistically high average Signal-to-Noise Ratio (SNR) of 50 dB is employed.

Throughput and BLER results are visualized in Figure 9. The curves denoted as *fast fading* represent the link level results. The straight line in Figure 9a, denoted as *BF 14 OFDM symbols without ICI*, has been obtained from system level simulations without adding ICI noise. In this case, the performance is *independent* of the user velocity. Adding ICI noise yields the curve denoted
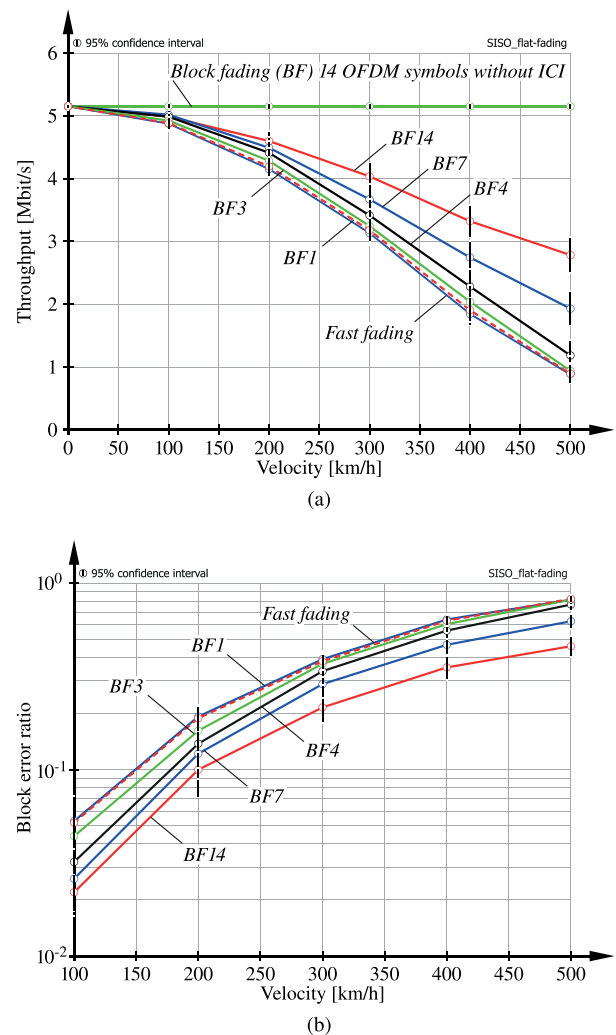

FIGURE 9. Throughput and BLER for fast fading channels and block fading channels with varying fading block-length: BFx corresponds to block fading over x OFDM symbols. ICI is considered as additional Gaussian noise. (a) Throughput reduction with growing user velocity. (b) BLER degradation with growing user velocity.

as *BF 14* (block fading over 14 OFDM symbols), which lies significantly above the fast fading link level result. Thus, ICI noise alone is *not sufficient* to realistically represent the performance of a fast fading channel.

C. SHORT BLOCK FADING

It is necessary to consider the increased temporal diversity of the channel by reducing the block-length of the block fading channel model. The results are illustrated by the remaining curves in Figure 9a. Figure 9b shows the corresponding BLER curves. It is observed that a fading block-length of at most three OFDM symbols should be employed to accurately reproduce the link level results. The shortening of the block-length is denoted as *short block fading*.

Activating ICI noise and selecting a fading block-length of three OFDM symbols for the system level simulation, we finally compare the throughput performance in a more complex scenario, where the eNodeB is equipped with
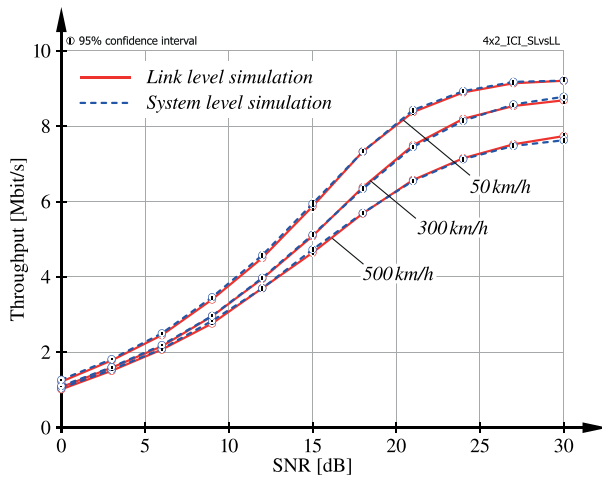
FIGURE 10. Comparison of the throughput for different user velocities as obtained from link- and system level simulations, respectively.

four transmit antennas and the UE has two receive antennas. The SNR is varied from 0 to 30 dB. We evaluate the throughput reduction with increasing user velocity, assuming that transmission rate adaptation is activated. The results of the link level simulation (red solid) and the system level simulation (blue dashed) are shown in Figure 10. We observe an accurate match between link level and system level, substantiating the validity of this simple ICI model. In this setup, the system level simulator was roughly $35\times$ faster.

Hence, the Vienna LTE-A system level simulator was extended to enable a reduced fading block-length, facilitating high-mobility simulations. This *short block fading* option, however, should be utilized deliberately, as it significantly increases the computational complexity of the simulations.

REFERENCES

[1] (Jan. 2015). *ITU-R Working Party 5D (WP 5D) Contributions*. [Online]. Available: http://www.itu.int/md/R07-WP5D-C/en

[2] E. Dahlman, S. Parkvall, and J. Skold, *4G: LTE/LTE-Advanced for Mobile Broadband*. Amsterdam, The Netherlands: Elsevier, 2011.

[3] S. Ahmadi, *LTE-Advanced: A Practical Systems Approach to Understanding 3GPP LTE Releases 10 and 11 Radio Access Technologies* (ITPro Collection). Amsterdam, The Netherlands: Elsevier, 2013.

[4] Y. Wang, J. Xu, and L. Jiang, "Challenges of system-level simulations and performance evaluation for 5G wireless networks," *IEEE Access*, vol. 2, pp. 1553–1561, 2014.

[5] M. Gerasimenko *et al.*, "Performance comparison of system level simulators for 3GPP LTE uplink," in *Internet of Things, Smart Spaces, and Next Generation Networking* (Lecture Notes in Computer Science), vol. 7469, S. Andreev, S. Balandin, and Y. Koucheryavy, Eds. Berlin, Germany: Springer-Verlag, 2012, pp. 186–197.

[6] (Jan. 2015). *Riverbed*. [Online]. Available: http://www.riverbed.com/products/performance-management-control/opnet.html?redirect=opnet

[7] (Jan. 2015). *OMNeT++*. [Online]. Available: http://www.omnetpp.org

[8] (Mar. 2015). *IT++*. [Online]. Available: http://itpp.sourceforge.net/4.3.1/

[9] (Jan. 2015). *ns-2*. [Online]. Available: http://www.isi.edu/nsnam/ns

[10] (Jan. 2015). *ns-3*. [Online]. Available: http://www.nsnam.org/

[11] (Jan. 2015). *GNS3*. [Online]. Available: http://www.gns3.com/

[12] S. Max, D. Bültmann, R. Jennen, and M. Schinnenburg, "Evaluation of IMT-advanced scenarios using the open wireless network simulator," in *Proc. Int. ICST Conf. Simulation Tools Techn.*, Torremolinos, Spain, Mar. 2010, p. 26.

[13] (Jan. 2015). *Hurricane II WAN Emulation and Network Simulation*. [Online]. Available: http://packetstorm.com/packetstorm-products/hurricane-ii-software

[14] (Jan. 2015). *Nomor System Level Simulation*. [Online]. Available: http://www.nomor.de/home/solutions-and-products/system-level-simulation

[15] D. Martín-Sacristán, J. F. Monserrat, V. Osa, and J. Cabrejas, "LTE-advanced system level simulation platform for IMT-advanced evaluation," *Waves*, 2011.

[16] Y. Li, F. Yu, S.-L. Zheng, and C.-L. Yang, "LTE system level simulation with MATLAB," in *Proc. Int. Conf. Internet Technol. Appl. (iTAP)*, Aug. 2011, pp. 1–4.

[17] G. Piro, L. A. Grieco, G. Boggia, F. Capozzi, and P. Camarda, "Simulating LTE cellular systems: An open-source framework," *IEEE Trans. Veh. Technol.*, vol. 60, no. 2, pp. 498–513, Feb. 2011.

[18] (Feb. 2015). *The Vienna LTE Simulators*. [Online]. Available: http://www.nt.tuwien.ac.at/ltesimulator

[19] Mathworks. (Jul. 2014). *MATLAB Documentation*. [Online]. Available: http://www.mathworks.com/help/matlab/index.html

[20] K. Abdallah, I. Cerutti, and P. Castoldi, "Energy-efficient coordinated sleep of LTE cells," in *Proc. IEEE Int. Conf. Commun. (ICC)*, Ottawa, ON, Canada, Jun. 2012, pp. 5238–5242.

[21] M. Carvalho and P. Vieira, "An enhanced handover oscillation control algorithm in LTE self-optimizing networks," in *Proc. IEEE Int. Symp. Wireless Pers. Multimedia Commun. (WPMC)*, Brest, France, Oct. 2011, pp. 1–5.

[22] M. M. Selim, M. El-Khamy, and M. El-Sharkawy, "Enhanced frequency reuse schemes for interference management in LTE femtocell networks," in *Proc. IEEE Int. Symp. Wireless Commun. Syst. (ISWCS)*, Paris, France, Aug. 2012, pp. 326–330.

[23] S. Y. Shin and D. Triwicaksono, "Radio resource control scheme for machine-to-machine communication in LTE infrastructure," in *Proc. Int. Conf. ICT Converg. (ICTC)*, Jeju Island, Korea, Oct. 2012, pp. 1–6.

[24] J. C. Ikuno, "System level modeling and optimization of the LTE downlink," Ph.D. dissertation, Vienna Univ. Technol., Vienna, Austria, 2013.

[25] *Evolved Universal Terrestrial Radio Access (E-UTRA); Further Advancements for E-UTRA Physical Layer Aspects*, 3rd Generation Partnership Project (3GPP), document Rec. TR 36.814, Mar. 2010.

[26] *Coordinated Multi-Point Operation for LTE Physical Layer Aspects*, 3rd Generation Partnership Project (3GPP), document Rec. TR 36.819, Sep. 2013.

[27] *Evolved Universal Terrestrial Radio Access (E-UTRA); Radio Frequency (RF) System Scenarios*, 3rd Generation Partnership Project (3GPP), document Rec. TR 36.942, Oct. 2014.

[28] *Guidelines for Evaluation of Radio Transmission Technologies for IMT-2000*, ITU Radiocommunication Sector (ITU-R), document Rec. ITU-R M.1225.

[29] P. Kyösti *et al.*, "WINNER II channel models," Tech. Rep., Sep. 2007. [Online]. Available: http://www.ist-winner.org/deliverables.html

[30] *Study on 3D Channel Model for LTE*, 3rd Generation Partnership Project (3GPP), document Rec. TR 36.873, Sep. 2014.

[31] R. W. Heath, Jr., M. Airy, and A. J. Paulraj, "Multiuser diversity for MIMO wireless systems with linear receivers," in *Proc. Conf. Rec. 35th Asilomar Conf. Signals, Syst. Comput.*, vol. 2. Nov. 2001, pp. 1194–1199.

[32] I. Latif, F. Kaltenberger, and R. Knopp, "Link abstraction for multi-user MIMO in LTE using interference-aware receiver," in *Proc. IEEE Wireless Commun. Netw. Conf. (WCNC)*, Apr. 2012, pp. 842–846.

[33] M. Döttling *et al.*, "Assessment of advanced beamforming and MIMO technologies," Tech. Rep. D2.7, May 2005.

[34] S. Caban, C. Mehlführer, and M. Wrulich, *Evaluation of HSDPA and LTE: From Testbed Measurements to System Level Performance*. New York, NY, USA: Wiley, 2011.

[35] Nortel Networks, *OFDM Exponential Effective SIR Mapping Validation, EESM Simulation Results*, 3rd Generation Partnership Project (3GPP), document Rec. R1-040089, Jan. 2004.

[36] S. Schwarz, M. Wrulich, and M. Rupp, "Mutual information based calculation of the precoding matrix indicator for 3GPP UMTS/LTE," in *Proc. Int. ITG Workshop Smart Antennas (WSA)*, Bremen, Germany, Feb. 2010, pp. 52–58.

[37] E. Björnson and E. Jorswieck, "Optimal resource allocation in coordinated multi-cell systems," *Found. Trends Commun. Inf. Theory*, vol. 9, nos. 2–3, pp. 113–381, 2013.

[38] *Study on Elevation Beamforming/Full-Dimension (FD) MIMO for LTE*, 3rd Generation Partnership Project (3GPP), document Rec. TR 36.897, Dec. 2014.

[39] S. Schwarz, J. C. Ikuno, M. Simko, M. Taranetz, Q. Wang, and M. Rupp, "Pushing the limits of LTE: A survey on research enhancing the standard," *IEEE Access*, vol. 1, pp. 51–62, 2013.

[40] B. Ai *et al.*, "Challenges toward wireless communications for high-speed railway," *IEEE Trans. Intell. Transp. Syst.*, vol. 15, no. 5, pp. 2143–2158, Oct. 2014.

[41] R. He, Z. Zhong, B. Ai, G. Wang, J. Ding, and A. F. Molisch, "Measurements and analysis of propagation channels in high-speed railway viaducts," *IEEE Trans. Wireless Commun.*, vol. 12, no. 2, pp. 794–805, Feb. 2013.

[42] L. Gao, Z. Zhong, B. Ai, and L. Xiong, "Estimation of the Ricean factor in K the high speed railway scenarios," in *Proc. Int. ICST Conf. Commun. Netw. China*, Aug. 2010, pp. 1–5.

[43] M. K. Müller, M. Taranetz, and M. Rupp. (2015). "Providing current and future cellular services to high speed trains." [Online]. Available: http://arxiv.org/abs/1505.04557

[44] M. K. Müller, M. Taranetz, and M. Rupp, "Performance of remote unit collaboration schemes in high speed train scenarios," in *Proc. IEEE Veh. Technol. Conf. (VTC)*, Boston, MA, USA, Sep. 2015.

[45] C. D. Gavrilovich, Jr., "Broadband communication on the highways of tomorrow," *IEEE Commun. Mag.*, vol. 39, no. 4, pp. 146–154, Apr. 2001.

[46] H. Kopetz, "Internet of Things," in *Real-Time Systems* (Real-Time Systems Series). New York, NY, USA: Springer-Verlag, 2011, pp. 307–323.

[47] M. Simko, P. S. R. Diniz, Q. Wang, and M. Rupp, "Adaptive pilot-symbol patterns for MIMO OFDM systems," *IEEE Trans. Wireless Commun.*, vol. 12, no. 9, pp. 4705–4715, Sep. 2013.

[48] Y.-S. Choi, P. Voltz, and F. A. Cassara, "On channel estimation and detection for multicarrier signals in fast and selective Rayleigh fading channels," *IEEE Trans. Commun.*, vol. 49, no. 8, pp. 1375–1387, Aug. 2001.

MARTIN TARANETZ (S'07) received the B.Sc. degree in electrical engineering and Dipl.-Ing degree (M.Sc. equivalent) in telecommunications with highest honors from the TU Wien, Vienna, Austria, in 2008 and 2011, respectively. He is currently pursuing the Ph.D. degree in telecommunications engineering and he is employed as a University Assistant with the Institute of Telecommunications, TU Wien. From 2014 to 2014, he was a Visiting Researcher with the Wireless Networking and Communications Group, The University of Texas at Austin. His research interests lie in the fields of wireless communications and signal processing. In his Ph.D. thesis, he focuses on system level modeling and evaluation of heterogeneous cellular networks. He is a Reviewer for IEEE TRANSACTIONS ON WIRELESS COMMUNICATIONS and the IEEE TRANSACTIONS ON SIGNAL PROCESSING.

THOMAS BLAZEK received the B.Sc. degree in electrical engineering from the TU Wien, Vienna, Austria, in 2013. He is currently pursuing the M.Sc. degree in telecommunications engineering. He is employed as a Project Assistant at the Institute of Telecommunications, TU Wien, focusing on vehicular connectivity. His current research topics include modeling and analysis of vehicular channels.

THOMAS KROPFREITER received the B.Sc. degree in electrical engineering and the Dipl.-Ing degree (M.Sc. equivalent) in telecommunication engineering from the TU Wien, Vienna, Austria, in 2012 and 2014, respectively. His Diploma thesis dealt with a quantization of soft information in distributed hypothesis testing scenarios. From 2013 to 2015, he was a member of the Mobile Communications Group, TU Wien, where he worked on the topic of beamforming in multicell scenarios. Since 2015, he has been employed as a Project Assistant at TU Wien, where he is currently pursuing the Ph.D. degree. His current research interests are random finite sets in the field of target tracking and self localization.

MARTIN KLAUS MÜLLER (S'13) received the B.Eng. degree in electrical and telecommunication engineering from the DHBW Ravensburg, Friedrichshafen, in cooperation with Rohde and Schwarz, in 2009, and the Dipl.-Ing degree (M.Sc. equivalent) in telecommunications from the TU Wien, Vienna, Austria, in 2013. His Diploma thesis focused on feedback based LTE-A measurements. He is currently pursuing the Ph.D. degree in telecommunications engineering and he is employed as a Project Assistant with the Institute of Telecommunications, TU Wien. His current research interests include mobile cellular access in train- and highway scenaros and wireless communication in indoor-scenarios.

STEFAN SCHWARZ (S'10–M'14) received the B.Sc. degree in electrical engineering and the Dipl.-Ing. degree (M.Sc. equivalent) in telecommunications engineering with highest distinctions in 2007 and 2009, respectively, both at the TU Wien, and the Dr.techn. degree (Ph.D. equivalent) in telecommunications engineering with highest distinctions at the TU Wien, in 2013. In 2010, he received the honorary price of the Austrian Minister of Science and Research, for excellent graduates of scientific and artistic universities, and in 2014, he received the INiTS Award in the category Information and Communication Technologies for his dissertation on Limited Feedback Transceiver Design for Downlink MIMO OFDM Cellular Networks. Since 2008, he has been a Project Assistant with the Mobile Communications Group, Institute of Telecommunications, TU Wien. His research interests are located in the broad fields of wireless communications and signal processing. In his dissertation, he focused on limited feedback single- and multiuser MIMO-OFDM communication systems, and multi-user scheduling algorithms. He actively serves as a Reviewer of the IEEE TRANSACTIONS ON COMMUNICATIONS, SIGNAL PROCESSING, WIRELESS COMMUNICATIONS AND VEHICULAR TECHNOLOGY, *EURASIP Journal on Signal Processing*, and *Journal on Wireless Communications and Networking*.

MARKUS RUPP received the Dipl.-Ing. degree at the University of Saarbrücken, Germany, in 1988, and the Dr.-Ing. degree from the Technische Universität Darmstadt, Germany, in 1993, where he worked with Eberhardt Hänsler on designing new algorithms for acoustical and electrical echo compensation. From 1993 to 1995, he had a post-doctoral position with the University of Santa Barbara, California, with S. Mitra, where he worked with A. H. Sayed on a robustness description of adaptive filters with impact on neural networks and active noise control. From 1995 to 2001, he was a member of Technical Staff with the Wireless Technology Research Department, Bell-Labs, Crawford Hill, NJ, where he worked on various topics related to adaptive equalization and rapid implementation for IS-136, 802.11, and UMTS. Since 2001, he has been a Full Professor of Digital Signal Processing in Mobile Communications at the TU Wien, where he served as the Dean from 2005 to 2007. He was an Associate Editor of the IEEE TRANSACTIONS ON SIGNAL PROCESSING from 2002 to 2005, where he is currently an Associate Editor of *JASP EURASIP Journal of Advances in Signal Processing*, and *JES EURASIP Journal on Embedded Systems*. He has been elected as a AdCom Member of EURASIP since 2004 and serving as the President of EURASIP from 2009 to 2010. He has authored or co-authored over 500 scientific papers, including 15 patents on adaptive filtering, and wireless communications.

• • •